Physics Letters A 374 (2010) 4589–4593

Contents lists available at ScienceDirect

Physics Letters A

www.elsevier.com/locate/pla

Experimental bifurcation diagram of a circuit-implemented neuron model

D. Linaro, T. Poggi, M. Storace *

Biophysical and Electronic Engineering Department, University of Genoa, Via Opera Pia 11a, I-16145 Genova, Italy

ARTICLE INFO

Article history:
Received 28 July 2010
Received in revised form 16 September 2010
Accepted 17 September 2010
Available online 21 September 2010
Communicated by C.R. Doering

Keywords:
Experimental bifurcation diagram
Hardware neuron model
Classification algorithm

ABSTRACT

An experimental bifurcation diagram of a circuit implementing an approximation of the Hindmarsh–Rose (HR) neuron model is presented. Measured asymptotic time series of circuit voltages are automatically classified through an *ad hoc* algorithm. The resulting two-dimensional experimental bifurcation diagram evidences a good match with respect to the numerical results available for both the approximated and original HR model. Moreover, the experimentally obtained current–frequency curve is very similar to that of the original model. The obtained results are both a proof of concept of a quite general method developed in the last few years for the approximation and implementation of nonlinear dynamical systems and a first step towards the realisation *in silico* of HR neuron networks with tunable parameters.

1. Introduction

Among the most active trends in neuroscience are both studying the behaviour of neuronal networks and modelling/emulating realistically such networks. Obviously, such an effort must be carried out jointly in different fields of science, such as biology, physics, neuroscience, mathematics, computer science, and electronics. In this kind of research activity, it is commonplace to combine experimental studies of animal and human nervous systems with numerical simulations of mathematical models [1]. Despite the fact that huge efforts have been put into the simulation of realistic neuron networks [2] and the abundance of software simulators [3,4], also a completely different approach has attracted the attention of many scientists: the hardware implementation of neurons and neuron networks. The main disadvantage of a custom hardware solution is that the implementation of a circuit whose behaviour emulates accurately another physical system is an articulated process, whose careful completion requires usually much more time than writing code for computer simulations. Concerning the main advantages of a hardware neuron, the ordinary differential equations (ODEs) defining the model are solved in real time by the circuit and the time scale of the circuit dynamics can be properly changed by operating on some circuit parameters, e.g., capacitances. When implementing networks, the main advantage of a hardware realisation is its intrinsically parallel structure. Moreover, hardware neuron networks can be interconnected either among them, to realise more complex networks, or with real neuron networks [5]. For a systematic review about hybrid analogue/digital models, with pros and cons, the reader is referred to [6].

Nowadays, there exist circuit implementations of both neuron models with a high level of abstraction, such as integrate-and-fire models (see [7,8] and references therein) that allow the realisation of networks with thousands of neurons, and more biologically plausible models (see [9–11] and references therein), which can be exploited to implement more specialized but smaller networks (with few up to tens of neurons), such as central pattern generators. In both cases, tuning the parameters of each neuron is often a cumbersome and error prone task. An experimental bifurcation diagram can provide guidelines to tune the parameters of a given hardware neuron in order to obtain the desired dynamics [12,13].

For the rest of this Letter, we shall focus on the Hindmarsh–Rose (HR) neuron model [14]: its vector field contains only polynomial nonlinearities and depends on various parameters that allow reproduction of the main dynamical behaviours exhibited by biological neurons, such as spike frequency adaptation and stationary, spiking, bursting, and chaotic regimes. The HR model has attracted the attention of scientists oriented to its electronic synthesis [15,16] as well as researchers interested in its analysis (see [17–19] and references therein). Unfortunately, these two aspects are still separated and, to the best of the authors' knowledge, no systematic analysis of the behaviours that can be obtained in the hardware model by acting on system parameters has been presented. The global bifurcation scenario of a given circuit may be useful in more biophysically oriented studies, for instance as a guide to choose the parameters for fitting the implemented model to qualitatively different types of electrophysiological behaviours [20] and then to implement small specialized networks.

* Corresponding author.
E-mail addresses: daniele.linaro@unige.it (D. Linaro), tomaso.poggi@unige.it (T. Poggi), marco.storace@unige.it (M. Storace).

0375-9601/$ – see front matter
doi:10.1016/j.physleta.2010.09.030

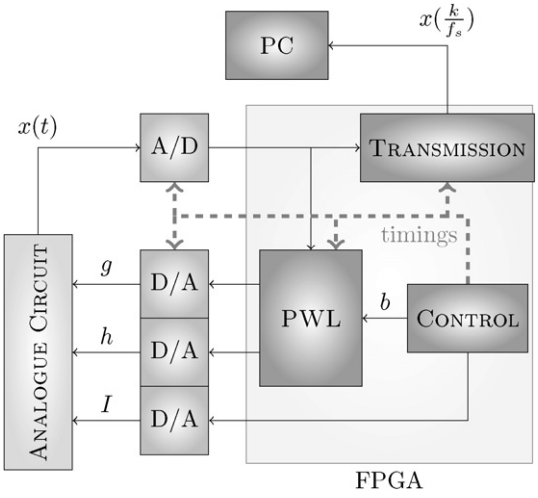

Fig. 1. Block scheme of the experimental setup.

In this contribution, we propose a two-dimensional experimental bifurcation diagram of an electronic circuit implementing an approximation of the HR model [21]. The diagram is obtained through automatic acquisition and classification of the experimental measurements. Since our goal is to provide qualitative and quantitative guidelines to tune two circuit parameters to reproduce a desired neuron behaviour (corresponding to a stable solution), we will not focus on bifurcation curves, but instead on the interior of the regions delimited by these curves, where the circuit behaviour is structurally stable [22]. The obtained bifurcation diagram evidences a good matching with respect to the numerical results available for both the approximated and original HR model. Moreover, the experimentally obtained current–frequency curve – which is a characteristic feature of neuron models – matches the corresponding curve of the original HR model.

The proposed results are important not only in view of the hardware implementation of small networks of HR neurons, but also as a proof of concept of the reliability of the method for the approximation and circuit implementation of nonlinear dynamical systems described in [23].

2. Material and methods

The HR model is described by the following set of ODEs:

$$\begin{cases} \dot{x} = y - x^3 + bx^2 + I - z, \\ \dot{y} = 1 - 5x^2 - y, \\ \dot{z} = \mu\big(s(x - x_{rest}) - z\big), \end{cases} \tag{1}$$

in which we have fixed $\mu = 0.01$, $s = 4$, $x_{rest} = -1.6$. In the electronic circuit [21] we analyse in this Letter, which implements an approximation of system (1), the bifurcation parameters I and b can be varied within the ranges $[2, 6]$ and $[2.6, 3.5]$, respectively.

When a mathematical model is available, one can find the bifurcation diagram directly from the equations, by using brute-force approaches or continuation methods or both [24]. In order to have robust design criteria for a structurally stable circuit implementation of a neuron model, the quantitative results of the bifurcation analysis must be verified experimentally, against the unavoidable mismatches between the behaviours exhibited by a real system and by its mathematical model. In an experimental setup, the bifurcation diagram must be mapped out from measurements: as in [25], we use long time series recordings of one of the state variables for values of the parameters on a regular grid in the parameter plane (b, I).

With respect to the circuit presented in [21], both the digital and the analogue parts have been redesigned. The digital part – implemented on a Field Programmable Gate Array (FPGA) – has been programmed in order to automatically sweep a regular grid in the parameter plane.

The analogue part has been modified to reduce discrepancies between the dynamics of the model and that of the circuit: low-tolerance components have been used (in particular, capacitors with 1% tolerance); powering circuitry has been redesigned in order to keep analogue and digital supplies separated; second-order filters are now employed in the analogue-to-digital and digital-to-analogue conversion processes.

The digital part of the whole system is presented schematically in Fig. 1 and is made up of the following blocks: PWL provides piecewise-linear approximations (labelled as g and h) of the model nonlinear terms ($x^3 - bx^2$ and $5x^2$, respectively), depending on both the state variable x and the parameter b[1]; TRANSMISSION samples the signal $x(t)$ with frequency f_s and sends the data to a PC through a serial cable (the RS232 protocol has been used); CONTROL sets the values of the parameters b and I and manages the timings of the overall system. The sampling frequency f_s has been set to the maximum value allowed by the baud rate requirements of the RS232 protocol. Indeed, each sample is transmitted as a sequence of 11 bits (8 bits represent the data and 3 are control bits) at a frequency of 115.2 kHz. Since it is possible to send only one sample at a time, we set $f_s = \frac{115.2}{11}$ kHz $\simeq 10.5$ kHz. Then, after digitalisation, the time variable becomes k/f_s, with k integer.

The dashed lines denote control signals. The block CONTROL waits for a reset signal, sets a value for (b, I), waits 0.3 s to allow the circuit to reach asymptotic behaviour and then activates the TRANSMISSION block. When $T = 20\,000$ samples have been transmitted (corresponding to a measured time series that is about 2.3 s long), CONTROL changes the pair (b, I) and the process is repeated. The circuit is programmed to generate a regular grid of points on the parameter plane region $[2.6, 3.5] \times [2, 6]$ with steps $4.4 \cdot 10^{-3}$ and $25.6 \cdot 10^{-3}$ along the b and I directions, respectively.

Fig. 2 shows some examples of measured time series: it is evident that all the main dynamics of a neuron (spiking, bursting, and chaos, besides quiescence, which is not displayed) can be obtained with the proposed circuit. We performed a sweep in the parameters' plane in order to evidence stable invariant sets. In particular, b is increased linearly from 2.5 to 3.5 and, for each value of b, I is swept from the maximum (6) to the minimum (1).

On the other side of the communication channel, the PC receives the data and stores the experimental measurements (time series) corresponding to different pairs (b, I) into a text file. Once the data have been stored, we estimate the power spectral density of each time series in order to calculate its maximum bandwidth. In the worst case, the 99% of the power is confined below 700 Hz, which is far from the sampling frequency. Then, each recorded time series is low-pass filtered with a cut-off frequency of 2 kHz, to clear spurious frequency components.

3. Classification algorithm

The bifurcation diagram is obtained by automatically classifying the measurements. The classification is obtained by applying standard techniques to detect maxima of the time series (see, e.g., [25]). Particular attention is devoted to the classification of periodic dynamics, as described in the following. It is important to note that our classification algorithm differs from that presented in [25] in that we have no *a priori* information on the duration

[1] We do not dwell upon the approximation problem, which has been treated elsewhere. The interested reader is referred to [24] and references therein.

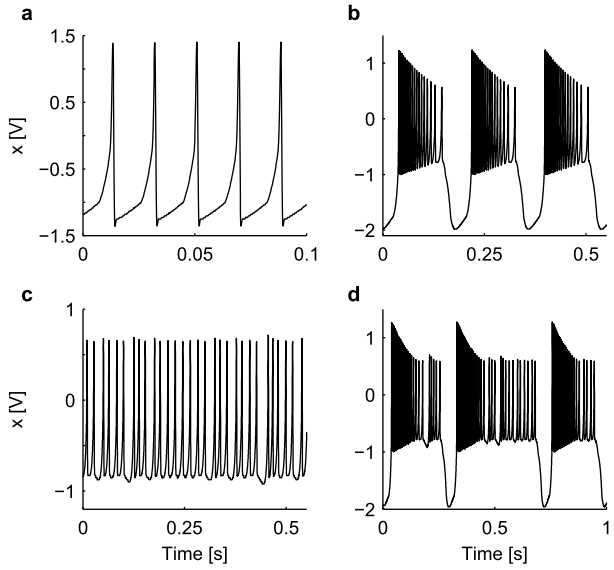

Fig. 2. Some examples of measured time series: (a) spiking ($b = 3.30$, $I = 4.50$), (b) bursting with 18 spikes per burst ($b = 2.55$, $I = 5.26$), (c) irregular (chaotic) spiking ($b = 2.60$, $I = 5.52$) and (d) irregular (chaotic) bursting ($b = 2.54$, $I = 5.57$).

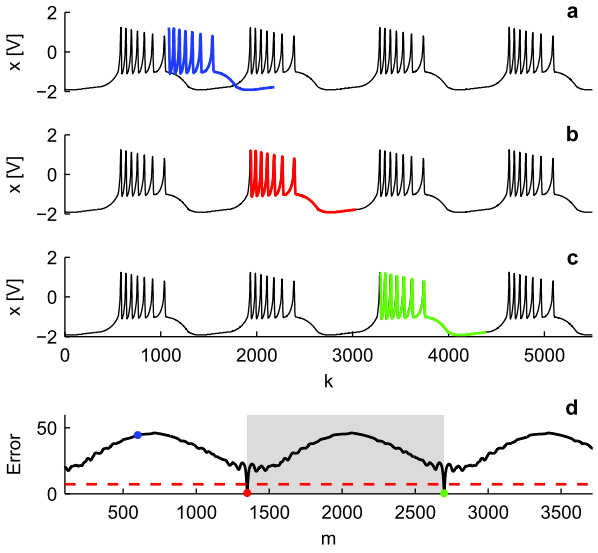

Fig. 3. An example of classification of a time series, where the colour traces highlight the sliding window: the blue trace in panel a shows no alignment (high value of error in panel d); the red trace in panel b and the green trace in panel c are correctly aligned (low error in panel d): this indicates that the green trace is displaced by the duration of a period with respect to the red trace in panel b. The shadowed area in panel d indicates the duration of the period. (For interpretation of colours in this figure, the reader is referred to the web version of this Letter.)

of the period, which can vary greatly for different parameters values. In other papers (see, e.g., [26]) experimental bifurcation curves are sketched starting from experimental measurements, but the method used to classify the time series is not discussed.

The algorithm first checks if the time series is either stationary or chaotic: the former behaviour is detected by verifying that the variations of the time series are within a range of 120 mV, while the non-quiescent solutions oscillate at least in the range $[-1, 1]$ V, as shown in Fig. 2. The classification of a chaotic time series is based on the fact that chaotic signals have a continuous "noiselike" broad power spectrum.

If none of these behaviours is detected, the time series is classified as periodic. In this case, the aim of the classification procedure is to detect the periodicity of the time series, i.e., the duration of a period and the number of maxima contained in each period.

Notwithstanding the initial filtering, the noise level (due to measurement and quantisation) still limits the reliable detection of (relative) maxima. Then, to detect the number of peaks in one single period, we apply the following steps (illustrated by the example shown in Fig. 3) to each time series:

1. Consider a time window of 0.15 s comprising $M = T/10 = 2000$ samples approximately; notice that the choice of M is such that a reasonable number (at least 3) of local maxima of the state variable falls in the observation window: this is done to avoid matches between single spikes when the neuron is showing more complex behaviours, like bursting.
2. Slide the window along the time series over the whole time course of x, with a step equal to $1/f_s$. In the upper three panels of Fig. 3, the black trace is the whole time series, whereas the coloured traces evidence the moving window. In particular, the blue trace in panel a is the window displaced by $m = 600$ samples, the red trace in panel b and the green trace in panel c are displaced by $m = 1350$ and $m = 2700$ samples, respectively, and match almost exactly the time series.
3. For each step, compute the discrepancy between the two time series as $E_m = \sum_{k=1}^{M} (x(\frac{k}{f_s}) - x(\frac{k+m}{f_s}))^2$, where $m = 0, \ldots, T - M$. Notice that, as shown in Fig. 3, when the time series is periodic, the error is periodic as well.
4. We determine the period of the time series x as the time difference between two local minima of E_m lower than a threshold defined as follows. Since E_m is periodic, we consider only local minima lower than $E = E_{\min} + 0.15(E_{\max} - E_{\min})$, with $E_{\min}$ and $E_{\max}$ the absolute minimum and maximum values of the error E_m, respectively. Notice that the threshold E (dashed line in panel d) is used to avoid considering local minima of E_m corresponding to the spikes of x in each period. In panel d, the blue, red and green dots indicate the values of E_m corresponding to panels a, b, and c respectively. It is evident that the green trace is displaced with respect to the red one by a period of the time series.
5. By counting the number of local maxima (peaks) of x in one period, we are able to correctly classify the trace. In the example shown in Fig. 3, for instance, the trace is classified as bursting with 7 spikes per burst.

4. Results and discussion

Fig. 4 shows the bifurcation diagrams for the original model (panel a), the piecewise-linear (PWL) approximated model (panel b) and the circuit (panel c), in which different colours have been associated with different asymptotic behaviours.

We have chosen to show the bifurcation diagrams only in the region $[2.6, 3.3] \times [2, 5]$ since it is the most interesting from the model dynamics standpoint: outside of this region (but within the region $[2.6, 3.5] \times [2, 6]$) the only observed behaviours are spiking and quiescence.

For a discussion about the bifurcation analysis of the original HR model and of its PWL approximation, the reader is referred to [24]. Here, we just point out the good qualitative matching among the three bifurcation diagrams. We also notice that we do not explicitly find out bifurcation curves (as in [25]), since the reference bifurcation structure is well known. Moreover, most bifurcation curves in the considered parameter region involve unstable invariant sets, which are not evident in the brute-force bifurcation diagram.

Fig. 5 shows two sets of time series obtained by integrating the original model Eq. (1) (black traces) and by measuring the output of the circuit (red traces) in the spiking region, for $b = 3.5$.

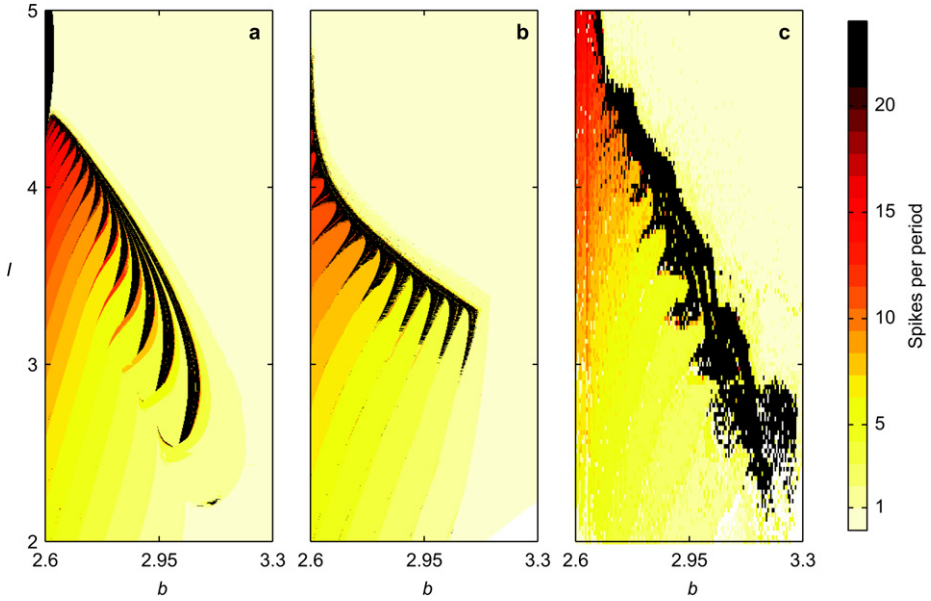

Fig. 4. Bifurcation diagrams: original model (a), PWL approximation (b), circuit (c). Different colours code different asymptotic behaviours: quiescence (white), spiking (light yellow), bursting (yellow, changing to red as the number of spikes per burst increases), and irregular chaotic (black). (For interpretation of colours in this figure, the reader is referred to the web version of this Letter.)

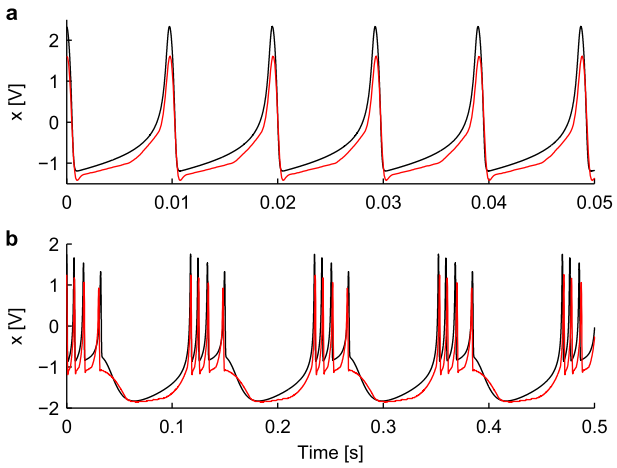

Fig. 5. Time series obtained by integrating the original model (black) and by measuring the state of the implemented circuit (red) in correspondence of different parameter pairs. (For interpretation of colours in this figure, the reader is referred to the web version of this Letter.)

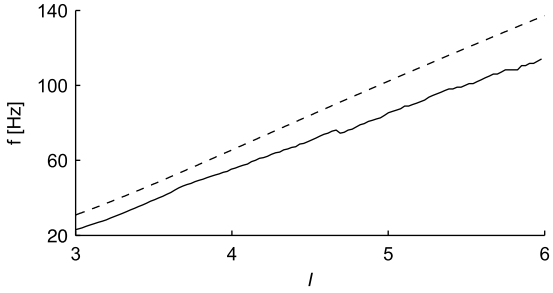

Fig. 6. Frequency versus injected current in the original model (dashed line) and its circuit implementation (solid line) for $b = 3.5$.

The control parameters b and I for the original model and for the circuit have been set to different values, in order to force the oscillations to have the same period. Thus, in panel a, we set $b = 3.4$ and $I = 5.05$ for the original model, $b = 3.4$ and $I = 5.95$ for the circuit; in panel b, we set $b = 2.8$ and $I = 2.25$ for the original model, $b = 2.9$ and $I = 2.85$ for the circuit. A desired dynamical behaviour present in the original model can be reproduced also in the implemented circuit by setting the parameters b and I in a neighbourhood of the nominal values. This fact is in accordance with the differences in the bifurcation diagrams shown in Fig. 4.

Fig. 6 shows the current–frequency curves obtained experimentally (solid line) and by simulation of the original model (1) (dashed line). It is evident that the linear relationship between frequency and current of the original model is preserved by the hardware implementation, albeit with an offset, which in general depends on the value of b.

5. Conclusions

The main results proposed in this Letter are two. Firstly, we have obtained a two-dimensional brute-force bifurcation diagram for a circuit implementing an approximation of the Hindmarsh–Rose neuron model: this diagram provides design rules to program the circuit in order to obtain the desired dynamics, both from a qualitative (on the basis of the colormap) and quantitative standpoints. From this latter point of view, one can find a pair of parameter values to match a given dynamic behaviour (obtained in the original model for a given (b^*, I^*) pair) by heuristic search in a neighbourhood of the point (b^*, I^*), also taking into account other available information: for instance, in the spiking region, the current–frequency curves suggest that to obtain the same spiking frequency as for the original model, in the circuit the parameter I must be set to a value higher than I^*, keeping $b = b^*$. To obtain the bifurcation diagram, we have developed a classification method that is suited for detecting the periodicity of neuronal signals. We remark that we have chosen the algorithm's parameters to tailor it to the particular case under analysis, but it could be used, with relatively low effort, to classify other membrane voltage traces.

The second, important result is the proof of the reliability of a method for the approximation and circuit implementation of nonlinear dynamical systems (based on PWL techniques), which

can be applied to obtain hardware realisations of different kinds of systems described by nonlinear ODEs. In this sense, this Letter constitutes the final step in the development, implementation and verification of a PWL version of the HR model, thus bridging the gap that still existed between the theoretical PWL approximation and its experimental proof.

Acknowledgement

Work partially supported by the European Commission through project MOBY-DIC (FP7-INFSO-ICT-248858), http://www.mobydic-project.eu.

References

[1] A. Herz, T. Gollisch, C. Machens, D. Jaeger, Science 314 (2006) 80.
[2] H. Markram, Nat. Rev. Neurosci. 7 (2) (2006) 153.
[3] N. Carnevale, M. Hines, The NEURON Book, Cambridge University Press, Cambridge, UK, 2006.
[4] M. Gewaltig, M. Diesmann, Scholarpedia 2 (4) (2007) 1430.
[5] J. Aliaga, N. Busca, V. Minces, G. Mindlin, B. Pando, A. Salles, L. Sczcupak, Phys. Rev. E 67 (2003) 061915.
[6] D. Luchinsky, P. McClintock, M. Dykman, Rep. Prog. Phys. 61 (1998) 889.
[7] D. Bruderle, E. Muller, A. Davison, E. Muller, J. Schemmel, K. Meier, Front. Neuroinf. 3 (2009) 17.
[8] G. Indiveri, E. Chicca, R. Douglas, Cognitive Comput. 1 (2) (2009) 119.
[9] J.D. Sitt, J. Aliaga, Phys. Rev. E 76 (2007) 051919.
[10] K. Hynna, K. Boahen, Neural Comput. 19 (2007) 327.
[11] Q. Zou, Y. Bornat, J. Tomas, S. Renaud, D. Destexhe, Neurocomputing 69 (2006) 1137.
[12] S. Binczak, S. Jacquir, J. Bilbault, V. Kazantsev, V. Nekorkin, Neural Networks 19 (2006) 684.
[13] A. Wagemakers, M. Sanjuan, J. Casado, K. Aihara, Int. J. Bifur. Chaos 16 (2006) 3617.
[14] J. Hindmarsh, R. Rose, Proc. R. Soc. Lond. Ser. B 221 (1984) 87.
[15] M. Denker, A. Szucs, R.D. Pinto, H.D.I. Abarbanel, A.I. Selverston, IEEE Trans. Biomed. Eng. 52 (5) (2005) 792.
[16] Y. Lee, J. Lee, K. Kim, Y. Kim, J. Ayers, Neurocomputing 71 (2007) 284.
[17] J.M. González-Miranda, Int. J. Bifur. Chaos 17 (2007) 3071.
[18] A. Shilnikov, M. Kolomiets, Int. J. Bifur. Chaos 18 (2008) 2141.
[19] G. Innocenti, R. Genesio, Chaos 19 (2009) 023124.
[20] E. de Lange, M. Hasler, Biol. Cybern. 99 (2008) 349.
[21] T. Poggi, A. Sciutto, M. Storace, Electron. Lett. 45 (2009) 966.
[22] Y. Kuznetsov, Elements of Applied Bifurcation Theory, 3rd edition, Springer-Verlag, New York, 2004.
[23] M. Storace, O. De Feo, IEEE Trans. Circ. Syst. I 51 (2004) 830.
[24] M. Storace, D. Linaro, E. de Lange, Chaos 18 (2008) 033128.
[25] S. Valling, B. Krauskopf, T. Fordell, A. Lindberg, Opt. Commun. 271 (2007) 532.
[26] S. Eriksson, Å.M. Lindberg, J. Opt. B: Quantum and Semiclassical Optics 4 (2002) 149.